Exploiting Symmetries for Efficient Postbuckling Analysis of Composite Plates

Ahmed K. Noor,* Michael D. Mathers,† and Melvin S. Anderson‡
NASA Langley Research Center, Hampton, Va.

Two aspects of the postbuckling analysis of composite plates are considered in this paper. The first pertains to identifying the different types of symmetry exhibited by the pre- and postbuckling responses of rectangular and skewed composite plates. A procedure is presented for exploiting these symmetries in finite-element and finite-difference analyses. The procedure can be used with existing programs having multipoint constraint capability. The second aspect pertains to the postbuckling response of biaxially loaded composite plates. Numerical results from finite-element analysis are presented that show the range of parameters for which shear deformation and/or anisotropy are important in buckling and postbuckling analysis.

Nomenclature

a_1, a_2 = side lengths of the plate
a = side length of a square plate
E_L, E_T = elastic moduli in the direction of fibers and normal to it, respectively
G_{LT}, G_{TT} = shear moduli in the plane of fibers and normal to it, respectively
h = thickness of the plate
$M_{\alpha\beta}$ = bending stress resultants ($\alpha, \beta = 1,2$)
$N_{\alpha\beta}$ = extensional (in-plane) stress resultants
N = uniform edge loading
p_α, p = external load intensities in the x_α and x_3 directions
Q_α = transverse shear stress resultants
U_{sh} = transverse shear strain energy
U_a = contribution of the anisotropic (nonorthotropic) terms to the strain energy of the plate
U_{tot} = total strain energy of the plate
u_α, w = displacement components in the coordinate directions
x_α, x_3 = Cartesian coordinate system (x_3 normal to the middle plane of the plate)
ϕ_α = rotation components
$[\Gamma]$ = transformation matrix
$\{\psi\}$ = nodal displacement and rotation components
$\kappa, \bar{\kappa}$ = constants that can have the values $+1$ and -1
θ = fiber orientation angle
ν_{LT} = major Poisson's ratio
$\partial_\alpha \equiv \partial/\partial x_\alpha$
[ ] = rectangular or square matrix
{ } = column matrix
$\mathcal{P}$, $\mathcal{L}$, $\mathcal{I}$ = dependent nodes obtained from the independent nodes by reflection in a plane, rotation of 180° about a line in the middle plane and inversion, respectively.

Subscripts

c,d = locations where displacements are measured

Received April 28, 1976; presented at the AIAA/ASME/SAE 17th Structures, Structural Dynamics, and Materials Conference, Valley Forge, Pa., May 5-7, 1976 (in bound volume of Conference papers, no paper number); revision received Sept. 27, 1976.

Index categories: Structural Stability Analysis; Structural Composite Materials.

*Professor of Engineering and Applied Science, George Washington University Center at NASA Langley Research Center. Member AIAA.

†Graduate Research Assistant, George Washington University Center at NASA Langley Research Center. Student Member AIAA.

‡Head, Analytical Methods Section, Structural Mechanics Branch, Structures and Dynamics Division. Member AIAA.

Introduction

ALTHOUGH considerable literature has been devoted to the postbuckling analysis of isotropic plates, investigations of laminated composite plates are rather few. Interest in the use of composite plates, manufactured from a number of individual unidirectional laminas, has recently been expanded in aircraft, shipbuilding, and other industries. Therefore, an understanding of their postbuckling response is desirable. In general, closed-form or analytic solutions cannot be obtained for the postbuckling problems. Therefore, it is usually necessary to resort to numerical or approximate solutions.

A number of approximate methods have been applied to the postbuckling analysis of composite plates in Refs. 1-7. Except for the study of the postbuckling response of uniaxially compressed sandwich plates reported in Ref. 3, all the other studies were based on the classical theory (with transverse shear deformation neglected).

Postbuckling analysis of composite plates is inhibited by the large number of parameters and the associated computational effort. A common way of reducing computational effort for the postbuckling analysis of isotropic and orthotropic plates is to take advantage of the symmetries present by imposing rather simple boundary conditions along lines of symmetry. For composite plates, anisotropic effects generally do not allow simple boundary conditions to be applied even though certain symmetries are clearly known and recognized. As a result, the full structure is often analyzed. The objectives of this paper are as follows:

1) To identify the different symmetries exhibited by the commonly used fibrous composite plates and to present a simple procedure for exploiting these symmetries in the finite-element postbuckling analysis; and,

2) To study the importance of transverse shear deformation and degree of anisotropy (nonorthotropy) in the postbuckling range for composite plates subjected to biaxial compression. Numerical results are presented for a large number of problems covering a wide range of lamination and geometric parameters of the plate.

The analytic formulation is based on a form of the geometrically nonlinear von Karman-type plate theory with the effects of transverse shear deformation, anisotropic material behavior, and bending-extensional coupling included. The composite shear correction factors presented in Ref. 8 are used.

A displacement (stiffness) finite-element formulation is used with the fundamental unknowns consisting of the displacement and rotation components of the middle plane of the plate u_α, w, and ϕ_α ($\alpha = 1,2$). The nodal parameters consist of the five generalized displacements at each node. The

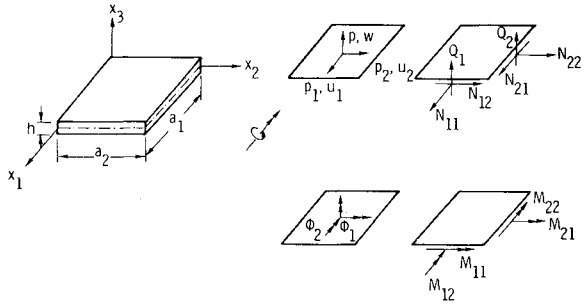

Fig. 1 Sign convention for stress resultants and generalized displacements.

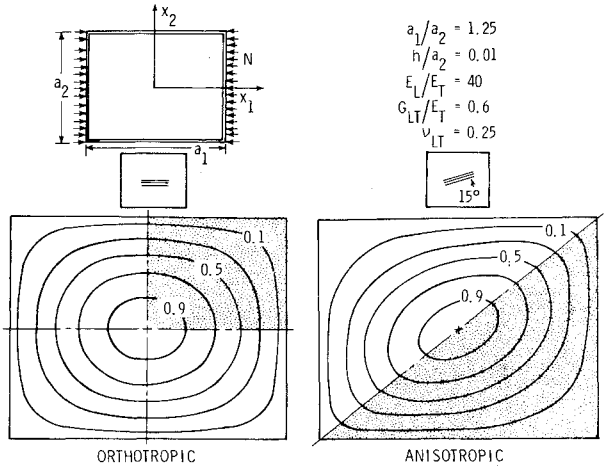

Fig. 2 Buckling mode shapes w/w_{max} for simply supported rectangular composite plates subjected to uniform axial compression.

sign convention for the different plate quantities is given in Fig. 1. The element stiffness matrix is obtained by minimizing the potential energy of the plate element. The details of the formulation are presented in Ref. 9 and are not reproduced herein. The stiffness matrices of the different elements are assembled and the resulting nonlinear algebraic equations are solved by the Newton-Raphson iterative technique. It should be emphasized, however, that the procedure outlined herein for exploiting the symmetries in the finite-element analysis can be readily used with other plate theories and other finite-element models (e.g., hybrid and mixed models).

II. Symmetries in Composite Plates

The contrast between the more familiar symmetries for orthotropic plates and those for composite plates having anisotropic properties is shown in Fig. 2. Contour plots for the buckling modes of a rectangular plate subjected to uniform longitudinal compression are shown for both orthotropic (fibers parallel to the x_1 axis) and anisotropic (fibers making 15° with the x_1 axis) material properties. The obvious lines of symmetry for the orthotropic plate can be used so that only one-quarter of the plate needs to be analyzed. The anisotropic plate also exhibits symmetry with respect to the midpoint. However, since no lines of symmetry exist, the usual procedure is to analyze the whole plate. As will be shown later, it is only necessary to model one-half of the plate. In Fig. 2, as well as in succeeding figures, the portion of the plate that needs to be analyzed is shown shaded. In this section, the symmetry relations that exist in composite plates will be identified and a method to reduce problem size will be presented.

The fundamental definitions of symmetry, symmetry elements, and symmetry operations are reviewed in Ref. 10. The axiom of symmetry introduced in Ref. 10 when applied to composite plates becomes the following: Given a composite

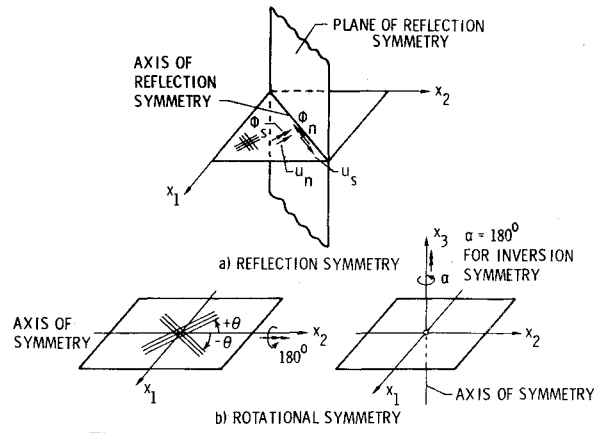

Fig. 3 Types of symmetry in composite plates.

plate exhibiting certain types of symmetry and a system of loads that exhibits the same types of symmetry as those of the plate, the response obtained will exhibit the same types of symmetry as those of the loading system. The symmetry of the plate refers to the symmetry of a) plate geometry, b) lamination parameters (e.g., fiber orientation and stacking of layers), and c) boundary conditions. The symmetry of the plate is described by giving the set of all reflections and rigid-body rotations and translations, which takes the plate into an equivalent configuration (i.e., into a configuration indistinguishable from the original configuration). Any such operation is called a *symmetry transformation*. The set of all symmetry transformations forms the *symmetry group* of the plate.[11]

The symmetry transformations of composite plates can all be built up from two fundamental types (see Fig. 3); namely, a) mirror reflection in a plane and b) rotation through a definite angle about an axis. The characteristics of these symmetries are examined subsequently.

Reflection Symmetry

A composite plate exhibits reflection symmetry (also called bilateral or mirror symmetry) with respect to a given plane if it can be brought into an equivalent configuration by mirror reflection in that plane (see Fig. 3). Obviously, the loading on the plate and the boundary conditions must possess mirror symmetry with respect to the same plane. Also, the fibers of the different layers must be either parallel or perpendicular to the plane of reflection symmetry. The symmetry relations that the loading components must satisfy for reflection symmetry with respect to the planes $x_1=0$, $x_2=0$, and $x_1=\pm x_2$ are given in Table 1. The corresponding symmetry (and antisymmetry) relations for the response variables (displacements and stress resultants) are given in Table 2.

Composite plates can possess one or more planes of reflection symmetry. An example of a composite plate exhibiting reflection symmetry is shown in Fig. 4. Figure 4 shows the buckling mode shapes for a composite square plate that is subjected to uniform biaxial compression and has one plane of reflection symmetry (plane $x_1=+x_2$). In this case it is only necessary to analyze one-half of the plate.

Note that the reflection symmetry relations listed in Table 2 are represented in the contour plots of Fig. 4, namely:

$$u_1(x_1,x_2)=u_2(x_2,x_1) \tag{1a}$$

$$u_2(x_1,x_2)=u_1(x_2,x_1) \tag{1b}$$

$$w(x_1,x_2)=w(x_2,x_1) \tag{1c}$$

Rotational Symmetry

A composite plate is said to exhibit rotational symmetry with respect to an axis if it can be brought into an equivalent

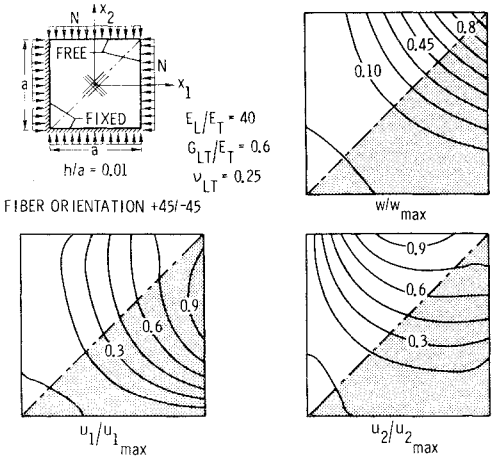

Fig. 4 Buckling mode shapes for a composite square plate with one plane of reflection symmetry subjected to uniform axial compression.

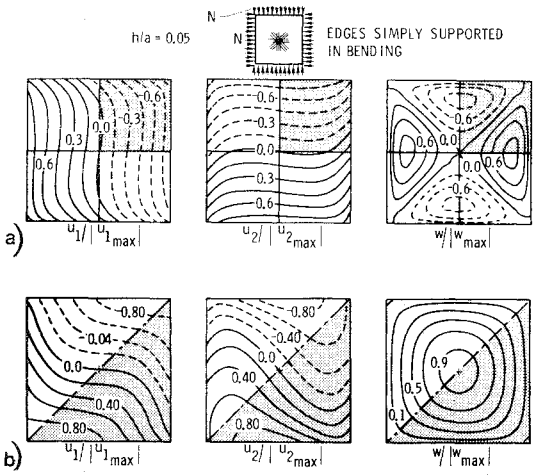

Fig. 5 Contour plots for prebuckling and postbuckling displacements. Four-layered quasi-isotropic square plate with fiber orientation 45/0/90/−45 subjected to uniform biaxial compression: a) Linear prebuckling displacements; b) Postbuckling displacements.

configuration by rotation around that axis. The axis of rotation is called an n-fold axis of symmetry if the smallest possible rotation, which takes the plate into an equivalent configuration, is $2\pi/n$ radians. An n-fold axis of symmetry has n symmetry operations associated with it, namely, rotations of 2π, π, $2\pi/3$,...$2\pi/n$.[10]

Rotational Symmetry $n=2$ with Respect to an Axis in the Middle Plane

Such a symmetry can be exhibited by the linear prebuckling response of composite plates having skew-symmetrical lamination with respect to their middle plane (Fig. 3). The symmetry relations for the loading components, generalized displacements, and stress resultants for rotational symmetry with respect to an axis $x_1=0$, $x_2=0$, and $x_1=\pm x_2$ are given in Tables 1 and 2.

Rotational Symmetry with Respect to a Line Normal to the Middle Plane of the Plate

The axis of rotation is assumed to coincide with the x_3 axis. A common form of this symmetry is axial symmetry that is exhibited by circular plates whose elastic characteristics, loading, and boundary conditions are independent of the circumferential coordinate.

For composite plates, rotational symmetry with $n=4$ (angle of rotation $=\pi/2$) is exhibited by the linear prebuckling

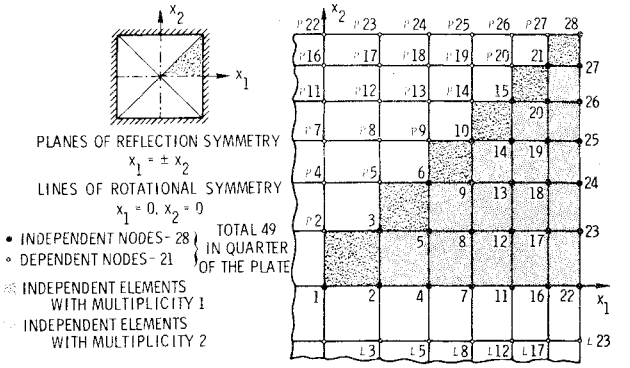

Fig. 6 Independent nodes and elements for composite plates with two planes of reflection symmetry and two lines of rotational symmetry.

response of quasi-isotropic plates with fiber orientations that are combinations of 45/0/90/−45, provided the plate geometry and loading exhibit the same type of symmetry. The symmetry relations for the loading, generalized displacements, and stress resultants are given in Tables 1 and 2. As an example for rotational symmetry with $n=4$, Fig. 5a shows contour plots for the prebuckling displacements of a square quasi-isotropic plate subjected to uniform biaxial compression. The symmetry relations listed in Table 2 are represented by the contour plots of Fig. 5a. In order for the symmetry relations to be applicable in the nonlinear range, the symmetry transformations must apply to the plate in its deformed state. A case where rotational symmetry with $n=4$ disappears in the postbuckling or nonlinear regime is demonstrated in Fig. 5b.

One of the most frequently encountered symmetries is rotational symmetry with $n=2$ (rotation angle $=\pi$) which is commonly called *inversion symmetry*. A composite plate exhibits inversion symmetry with respect to an axis x_3 normal to its plane if it can be brought into an equivalent configuration through 180° rotation about the axis. This amounts to changing the coordinates x_α of each material point of the plate into $-x_\alpha$. The x_3 axis is called the *axis of symmetry* and its intersection with the middle plane of the plate is called the *center of symmetry*.

The center of symmetry is located at the intersection of lines of geometric symmetry in the middle plane of the plate. For skew plates, the center of symmetry is located at the intersection of the two diagonals.

Inversion symmetry can be exhibited by both the prebuckling and postbuckling response of composite plates having arbitrary lamination, rectangular or skew planform provided the boundary conditions and loading exhibit this symmetry. An assembly of plate structures and/or shell structures can possess inversion symmetry, so that this type of symmetry will probably be most frequently used to reduce computational effort in the analysis of practical composite structures.

III. Exploiting Symmetries in Pre- and Postbuckling Analyses

Identifying the Symmetries

The first step in exploiting the symmetries inherent in composite plates in their pre- and postbuckling analyses is to identify these symmetries for a given plate geometry, lamination, and loading. This is accomplished by examining the plate for possible reflection, rotational or inversion symmetries. As the number of symmetries increases, the size of the mathematical model that needs to be analyzed is reduced. To illustrate the effect of lamination of the plate on the symmetries, Table 3 gives the symmetry transformations for composite rectangular plates having the following laminations: a) arbitrary lamination, b) cross ply ($\theta=0/90$) and angle ply ($\theta=\pm 45$),

Table 1 Symmetry relations for in-plane and transverse loading components[a]

	Mirror reflection in plane (or rotation with respect to line)				Rotational symmetry w.r.t. x_3 axis	
	$x_1 = 0$	$x_2 = 0$	$x_1 = +x_2$	$x_1 = -x_2$	n = 2 (inversion symmetry)	n = 4
$\begin{bmatrix} p_1 \\ p_2 \\ p \end{bmatrix}_{x_1,x_2} =$	$\begin{bmatrix} -p_1 \\ p_2 \\ \kappa p \end{bmatrix}_{-x_1,x_2}$	$\begin{bmatrix} p_1 \\ -p_2 \\ \kappa p \end{bmatrix}_{x_1,-x_2}$	$\begin{bmatrix} p_2 \\ p_1 \\ \kappa p \end{bmatrix}_{x_2,x_1}$	$\begin{bmatrix} -p_2 \\ -p_1 \\ \kappa p \end{bmatrix}_{-x_2,-x_1}$	$\begin{bmatrix} -p_1 \\ -p_2 \\ p \end{bmatrix}_{-x_1,-x_2}$	$\begin{bmatrix} -p_2 \\ p_1 \\ \bar{\kappa} p \end{bmatrix}_{x_2,-x_1}$

[a] $\kappa = -1$ for reflection in a plane and -1 for rotation with respect to a line. $\bar{\kappa} = +1$ for isotropic and -1 for quasi-isotropic plates. For antisymmetric (or skew-symmetric) response the entries in columns 2 through 6 must be multiplied by a minus sign.

Table 2 Symmetry relations for generalized displacements and stress resultants[a]

	Mirror reflection in plane (or rotation with respect to a line)				Rotational symmetry w.r.t. x_3 axis	
	$x_1 = 0$	$x_2 = 0$	$x_1 = +x_2$	$x_1 = -x_2$	n = 2 (inversion symmetry)	n = 4
Generalized displacements $\begin{bmatrix} u_1 \\ u_2 \\ w \\ \phi_1 \\ \phi_2 \end{bmatrix}_{x_1,x_2} =$	$\begin{bmatrix} -u_1 \\ u_2 \\ \kappa w \\ -\kappa\phi_1 \\ \kappa\phi_2 \end{bmatrix}_{-x_1,x_2}$	$\begin{bmatrix} u_1 \\ -u_2 \\ \kappa w \\ \kappa\phi_1 \\ -\kappa\phi_2 \end{bmatrix}_{x_1,-x_2}$	$\begin{bmatrix} u_2 \\ u_1 \\ \kappa w \\ \kappa\phi_2 \\ \kappa\phi_1 \end{bmatrix}_{x_2,x_1}$	$\begin{bmatrix} -u_2 \\ -u_1 \\ \kappa w \\ -\kappa\phi_2 \\ -\kappa\phi_1 \end{bmatrix}_{-x_2,-x_1}$	$\begin{bmatrix} -u_1 \\ -u_2 \\ w \\ -\phi_1 \\ -\phi_2 \end{bmatrix}_{-x_1,-x_2}$	$\begin{bmatrix} -u_2 \\ u_1 \\ \bar{\kappa} w \\ -\bar{\kappa}\phi_2 \\ \bar{\kappa}\phi_1 \end{bmatrix}_{x_2,-x_1}$
Stress resultants $\begin{bmatrix} N_{11} \\ N_{22} \\ N_{12} \\ M_{11} \\ M_{22} \\ M_{12} \\ Q_1 \\ Q_2 \end{bmatrix}_{x_1,x_2} =$	$\begin{bmatrix} N_{11} \\ N_{22} \\ -N_{12} \\ \kappa M_{11} \\ \kappa M_{22} \\ -\kappa M_{12} \\ -\kappa Q_1 \\ \kappa Q_2 \end{bmatrix}_{-x_1,x_2}$	$\begin{bmatrix} N_{11} \\ N_{22} \\ -N_{12} \\ \kappa M_{11} \\ \kappa M_{22} \\ -\kappa M_{12} \\ \kappa Q_1 \\ -\kappa Q_2 \end{bmatrix}_{x_1,-x_2}$	$\begin{bmatrix} N_{22} \\ N_{11} \\ N_{12} \\ \kappa M_{22} \\ \kappa M_{11} \\ \kappa M_{12} \\ \kappa Q_2 \\ \kappa Q_1 \end{bmatrix}_{x_2,x_1}$	$\begin{bmatrix} N_{22} \\ N_{11} \\ N_{12} \\ \kappa M_{22} \\ \kappa M_{11} \\ \kappa M_{12} \\ -\kappa Q_2 \\ -\kappa Q_1 \end{bmatrix}_{-x_2,-x_1}$	$\begin{bmatrix} N_{11} \\ N_{22} \\ N_{12} \\ M_{11} \\ M_{22} \\ M_{12} \\ -Q_1 \\ -Q_2 \end{bmatrix}_{-x_1,-x_2}$	$\begin{bmatrix} N_{22} \\ N_{11} \\ -N_{12} \\ \bar{\kappa} M_{22} \\ \bar{\kappa} M_{11} \\ -\bar{\kappa} M_{12} \\ -\bar{\kappa} Q_2 \\ \bar{\kappa} Q_1 \end{bmatrix}_{x_2,-x_1}$

[a] $\kappa = +1$ for reflection in a plane and -1 for rotation with respect to a line. $\bar{\kappa} = +1$ for isotropic and -1 for quasi-isotropic plates. For antisymmetric (or skew-symmetric) response the entries in columns 2 through 6 must be multiplied by a minus sign.

c) antisymmetric lamination with respect to the middle plane, and d) quasi-isotropic laminates with combinations of $\theta = 45/0/90/-45$. The loading on the plate and the boundary conditions are assumed to exhibit the same symmetries as those of the plate. For the purpose of comparison, the size of the mathematical model required for the analysis as well as the symmetry transformations for isotropic and homogeneous orthotropic rectangular plates are also given in Table 3. Some of the symmetries listed in Table 3 are not restricted to rectangular plates but can be exhibited by plates having other geometries (e.g., skew and polygonal plates). The symmetry relations for the generalized displacements and stress resultants implied by the symmetry transformations of Table 3 are given in Table 2.

Some of the symmetries present in the linear prebuckling response may disappear in the postbuckling response (e.g., rotational symmetry with respect to a line in the middle plane, see Table 3). Also, even though the prebuckling response of composite plates to a symmetric loading is symmetric, the postbuckling response can be either symmetric or antisymmetric. Unless one is certain about the response, one should consider making multiple analyses with both symmetric and antisymmetric modes in order not to miss the lower buckling modes. The antisymmetric modes can be determined from the same structural model with minor changes in input. The total number of analyses required might be as great as 2^k, where k is the number of symmetry transformations used in the analysis of the plate. However, the com-

Table 3 Symmetry transformations for composite rectangular plates [a]

Lamination type	Mirror reflection in plane (or rotation w.r.t. line)			Rotational symmetry w.r.t. x_3 axis		Size of model required	
	$x_1 = 0$	$x_2 = 0$	$x_1 = \pm x_2$ [b]	n = 4 [b]	n = 2 (inversion symmetry)	Square plate	Rectangular plate
Arbitrary laminate					•	1/2	1/2
Cross ply	•	•			•	1/4	1/4
Angle ply, $\theta = \pm 45$			•		•	1/4	1/2
Antisymmetric laminates: cross ply	•	•	o		•	1/8	1/4
Antisymmetric laminates: angle ply, $\theta = \pm 45$	o	o	•		•	1/8	1/4
Antisymmetric laminates: angle ply, $\theta \neq 45$	o	o			•	1/4	1/2
Quasi-isotropic (θ = + 45/0/90/- 45				o	•	1/4	1/2
Homogeneous orthotropic	•	•			•	1/4	1/4
Isotropic	•	•	•	•	•	1/8	1/4

[a] Symmetry transformation in this column applies to square plates.
[b] Solid circles for reflection in a plane and open circles for rotation with respect to a line. Symmetry transformations denoted by open circles do not apply to nonlinear problems.

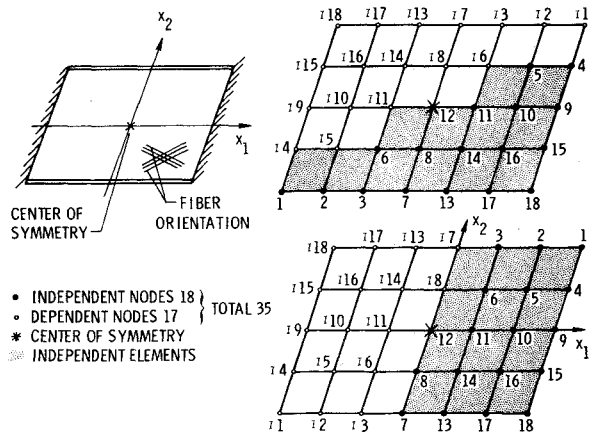

Fig. 7 Independent nodes and elements for composite skew plates with one center of inversion symmetry.

putational effort of these multiple analyses is usually less than that of a single analysis of the full plate.

Finite-Element Grids

In order to exploit the symmetries of composite plates in their analysis, the finite-element grid chosen *must* exhibit the same types of symmetry as those of the plate. This means that the grid can be brought into self-coincidence by each of the symmetry transformations used for the plate.

Independent Nodes and Elements

After the finite-element grid has been selected, the next step is to identify the nodes associated with the independent degrees of freedom of the plate. These nodes are referred to as *independent nodes*.[12] The other nodes in the plate are called *dependent nodes*. Henceforth, the dependent nodes are designated by the symbols $\mathcal{P}$, $\mathcal{L}$, and $\mathcal{I}$ according to whether they are obtained from independent nodes by reflection in a plane, rotation of 180° about a line in the middle plane, or inversion. Figures 6 and 7 show the independent and dependent nodes for composite plates with inversion and reflection symmetries.

The minimum number of finite elements which, by successive applications of symmetry transformations, can cover the whole plate will be referred to as the set of *independent elements*. Other elements will be called *dependent elements*. According to this definition, an independent element cannot be obtained from other independent elements by symmetry transformations (e.g., reflection or inversion).

The *multiplicity* of an independent element is defined as the number of times this element can appear in the plate by symmetry transformations. It is equal to one plus the number of dependent elements that can be obtained from that independent element by symmetry transformations. The size of

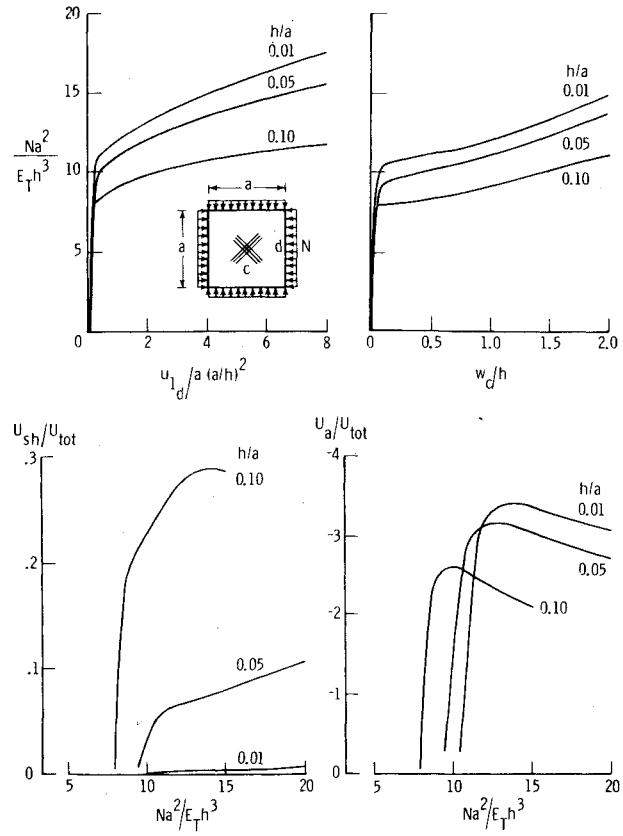

Fig. 8 Effect of h/a on postbuckling response of two-layered graphite-epoxy plate subjected to biaxial compression. Fiber orientation +45/−45.

the finite-element model and the number of simultaneous algebraic equations that are required in the analysis are governed by the number of independent elements and nodes, respectively. Note that independent nodes and elements are not uniquely given and can be selected in many different ways (see Fig. 7). However, the total number is independent of method of selection of independent elements.

A procedure for exploiting the symmetries of composite plates in their finite-element analysis has been presented in Ref. 12. In this section, a variation of this procedure is described that is suitable for use with existing finite-element and finite-difference programs with multipoint constraint capability such as the NASTRAN[13] and STAGS[5] programs. The two key elements in the procedure are outlined subsequently.

Modification of Element Stiffness and Load Matrices

If the independent elements in the analysis model have different multiplicities, the stiffness and load matrices of individual elements must be modified depending on their multiplicity. This can be easily accomplished in the input data if the values of the elastic moduli, shear moduli, as well as external loading of each independent element are multiplied by the ratio of the multiplicity of that element to the maximum multiplicity in the model. For inversion symmetry, this ratio will be equal to one for all elements and no modification is needed.

Application of Symmetry and Constraint Conditions

1) The boundary conditions along the edges of the independent elements are applied in the usual manner. In addition, the symmetry and skew-symmetry conditions must be applied at each of the centers of inversion symmetry and along the axes of reflection and rotational symmetry in the middle plane of the plate. The symmetry and skew-symmetry conditions for shear-flexible Lagrangian elements are listed in Table 4. For nodes lying on axes of reflection or rotational symmetry, the nodal parameters are selected to be the displacement and rotation components along and normal to those axes (see Table 4 and Fig. 3). This requires a corresponding transformation of the element stiffness and load matrices.

2) The degrees of freedom associated with the dependent nodes in the model *must* be related to those of the independent nodes by means of multipoint constraint conditions of the form

$$\{\psi\}_d = [\Gamma]\{\psi\}_i \tag{2}$$

where

$$\{\psi\}^T = [u_1 u_2 w\ \phi_1 \phi_2] \tag{3}$$

The vectors $\{\psi\}_d$ and $\{\psi\}_i$ are the dependent and corresponding independent degrees of freedom; $[\Gamma]$ is a transformation matrix. The forms of the $[\Gamma]$ matrices for a $\mathcal{P}$, $\mathcal{L}$, and $\mathcal{I}$ nodes are given in Appendix A. The foregoing procedure was found to result in considerable savings in the computational effort required for the analysis. Although no attempt was made to optimize solution time, experience for the cases presented herein showed savings of a factor of 2 for one-half models and a factor of 6 for one-fourth models.

IV. Postbuckling Behavior of Composite Plates

Numerical studies were conducted to investigate the effects of variations in the plate geometry, lamination parameters, and boundary conditions on postbuckling response as well as on the significance of shear deformation and degree of anisotropy (nonorthotropy) in composite plates.

A quantitative measure for the relative importance of transverse shear deformation at different load levels beyond buckling is taken to be the ratio of the transverse shear strain energy to the total strain energy of the plate U_{sh}/U_{tot}. The measure for the degree of anisotropy (nonorthotropy) is taken to be the ratio of the contribution of anisotropic (nonorthotropic) terms to the total strain energy of the plate U_a/U_{tot}. The two measures U_{sh}/U_{tot} and U_a/U_{tot} were first suggested and used in Ref. 8 for linear problems. These quantities will be shown for a number of different plates along with more familiar response variables such as transverse displacement and end shortening in order to assess the importance of transverse shear and anisotropy for a variety of parameters.

Square plates having both symmetric and skew-symmetric orientation with respect to the middle plane of the plate were considered. Also quasi-isotropic, four-layered plates were analyzed. The plates were subjected to uniform biaxial compression. The fiber orientation of the symmetric and skew-

Table 4 Symmetry and antisymmetry (or skew-symmetry) conditions for shear-flexible displacement finite element models.[a]

Center of inversion symmetry	Line of rotational symmetry[a]	Plane of reflection symmetry[a]
a) Symmetry Conditions		
$u_1 = u_2 = 0$	$u_n = 0$	$u_n = 0$
$\phi_1 = \phi_2 = 0$	$w = 0$	$\phi_n = 0$
	$\phi_s = 0$	
b) Skew-Symmetry Conditions		
$w = 0$	$u_s = 0$	$u_s = 0$
	$\phi_n = 0$	$w = 0$
		$\phi_s = 0$

[a] Subscripts *s* and *n* denote the tangential and normal components to the plane of reflection symmetry (or the axis of rotational symmetry), respectively.

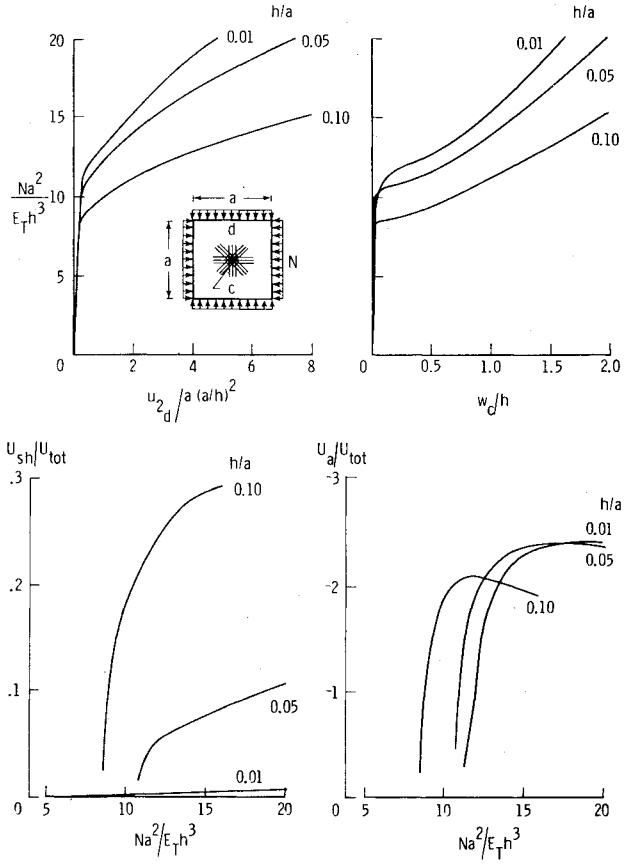

Fig. 9 Effect of h/a on postbuckling response of four-layered graphite-epoxy plate subjected to biaxial compression. Fiber orientation 45/0/90/−45.

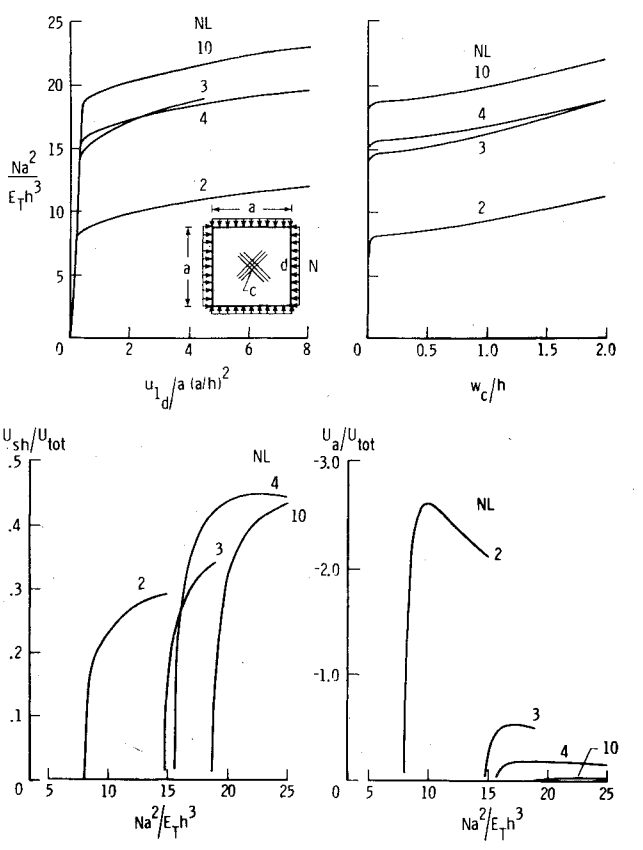

Fig. 10 Effect of number of layers *NL* on postbuckling response of graphite-epoxy square plate subjected to uniform biaxial compression. $h/a = 0.10$.

symmetric laminates alternate between +45 and −45 with respect to the x_1 axis. In the symmetric laminates, the +45 layers were at the outer surfaces of the laminate. The total thicknesses of the +45 and −45 layers in each laminate were the same. The quasi-isotropic laminates considered had fiber orientation of −45/90/0/45. All numerical solutions presented herein were obtained by using a higher-order, 16-node Lagrangian element and a 6×6 grid of elements in the full plate. A few runs were made with 4×4 and 8×8 grids to confirm that adequate convergence was achieved by using the 6×6 grid. In all solutions, advantage was taken of the symmetries exhibited by the plate. For plates with fiber orientation consisting of combinations of +45/−45, one-quarter of the plate was analyzed, and, for quasi-isotropic plates, only one-half of the plate was analyzed.

The material characteristics of the individual layers were taken to be those typical of high-modulus graphite-epoxy composites, namely

$$E_L/E_T = 40 \qquad G_{LT}/E_T = 0.6$$

$$G_{TT}/E_T = 0.5 \qquad \upsilon_{LT} = 0.25$$

where subscript L refers to the direction of fibers and subscript T refers to the transverse direction, υ_{LT} is the major Poisson's ratio. The edges of the plates are totally free to displace in the plane and are either simply supported or fixed with respect to bending. In addition to varying the boundary conditions, two parameters were varied, namely, the number of layers *NL* and the thickness ratio of the plate h/a, where h and a are the thickness and side length of the plate. The number of layers *NL* was varied between 2 and 10 and h/a was varied between 0.01 and 0.10. Typical results showing the effects of variations in a) the thickness ratio h/a, b) the number of layers *NL*, and c) the boundary conditions, on the response of the plate, as well as on the significance of shear deformation and degree of anisotropy are presented in Figs. 8-11. Each figure is in four parts, a load shortening curve, specifically load vs mid-side in-plane displacement curve, a plot of load as a function of the center transverse displacement, a plot of the transverse shear strain energies, and a plot of the contribution of the anisotropic terms to the strain energy. In each case the results for $h/a = 0.01$ are essentially unaffected by transverse shear and thus can be used as a basis for comparing the other curves in order to assess the effects of transverse shear. The load parameters used in all the curves is in the form of a buckling coefficient so that buckling would occur at the same value for all h/a if transverse shear was not present. Likewise, the strain parameter $u_{1_d}/a(a/h)^2$ is such that all load shortening curves are identical prior to buckling.

The load shortening curves show a sharp loss of axial stiffness after buckling compared to more familiar results of isotropic plates under uniaxial compression where a reduction of one-half is applicable. Part of this is due to the biaxial state of stress which increases the prebuckling stiffness but reduces the postbuckling stiffness. In addition, the mid-side edge displacement after buckling produced by a uniform biaxial stress field is significantly higher than the average edge displacement. In comparing the results for different values of h/a, it is seen that shear deformation has a significant effect on the buckling loads for plates with h/a of *0.05* and *0.1*. The plots of shear strain energy show a rapid increase in the vicinity of the buckling load. After buckling, the increase is more moderate with the exception of the results for clamped plates where the shear energy continues to grow at a rapid rate (Fig. 11). The curves for in-plane and transverse displacements for plates with $h/a = 0.05$ and *0.10* are nearly parallel to

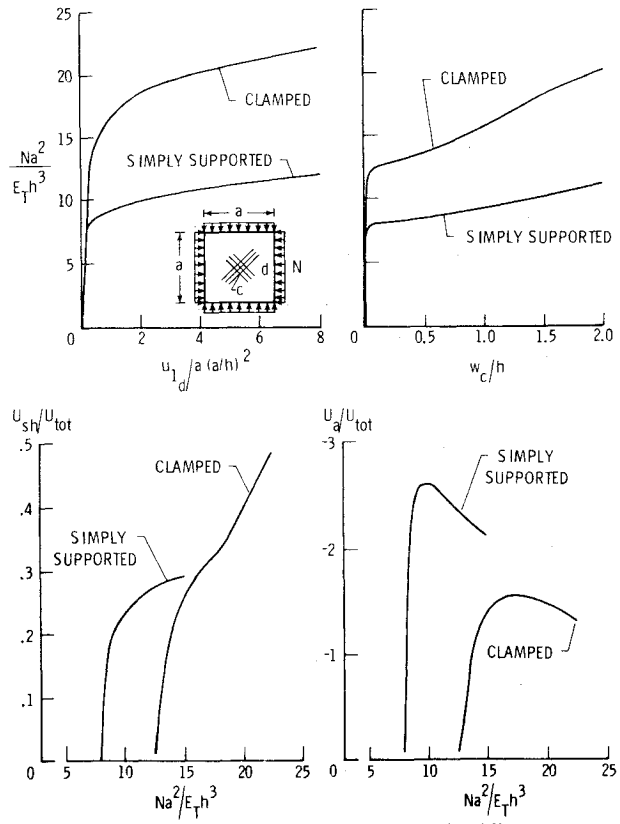

Fig. 11 Effect of boundary conditions on postbuckling response of two-layered skew-symmetrically laminated square plate subjected to uniform biaxial compression. $\theta = +45/-45$.

the corresponding curves for $h/a = 0.01$ (see Figs. 8 and 9). It thus appears that, for simply supported plates, if the effect of shear deformation on the buckling loads is not significant, it will not be important in the postbuckling range. However, the fact that the shear strain energy shows a moderate increase after buckling indicates that there is a transition range of h/a, where it may be necessary to include the shear deformation in the postbuckling range even though it was not important in the buckling analysis. This transition range is greater for clamped plates as indicated by the continued rise of the shear strain energy in Fig. 11.

As the number of layers increases, the degree of anisotropy decreases, and the buckling load increases. There is an associated increase in the shear strain energy for plates with higher buckling loads. Figure 10 shows that the curves of the in-plane and transverse displacements for the two-, three-, and four-layered plates are essentially parallel to the corresponding curves for 10-layered plates. This observation coupled with the fact that the degree of anisotropy shows a rapid increase at buckling, but little if any increase after buckling, suggests that anisotropic effects are important in the postbuckling range *only if* they are important in the buckling analysis.

V. Concluding Remarks

Two aspects of postbuckling analysis of composite plates are considered in this paper. The first pertains to identifying the different types of symmetry exhibited by the pre- and postbuckling responses of rectangular and skewed composite plates. A procedure is presented for exploiting these symmetries in the finite-element and finite-difference analyses. The procedure can be readily used with existing programs having multipoint constraint capability. Because the number of unknowns is typically reduced to about one-fourth or one-half of those for the full plate, considerable savings can result in the scope and cost of computations by using the proposed procedure. The second aspect pertains to the postbuckling response of composite plates. Numerical results are presented for composite plates subjected to uniform biaxial compression which show a pronounced loss of axial stiffness and a rapid increase of both the transverse shear deformation and degree of anisotropy after buckling. The shear deformation and degree of anisotropy in the postbuckling range are strongly dependent on the number and the stacking sequence of layers in addition to the degree of orthotropy of the individual layers and thickness ratio of the plate.

For simply supported composite square plates subjected to biaxial compression, the classical laminated plate theory is adequate for the postbuckling analysis of thin plates with $h/a < 0.05$. In addition, the orthotropic plate theory is adequate for multilayered angle-ply plates with $NL \geq 10$. In general, if the effects of transverse shear deformation and/or anisotropy on the buckling loads are not significant, they will not be important in the postbuckling analysis.

Appendix A. Transformation Matrix for $\mathcal{I}$, $\mathcal{P}$, and $\mathcal{L}$ Nodes

The transformation matrix $[\Gamma]$ at an $\mathcal{I}$ node is given by

$$[\Gamma] = \begin{bmatrix} -1 & & & & \\ & -1 & & & \\ & & +1 & & \\ & & & -1 & \\ & & & & -1 \end{bmatrix} \tag{A1}$$

If the plane of reflection symmetry (or the line of rotational symmetry) is $x_1 = x_2$, the matrices $[\Gamma]$ at $\mathcal{P}$ and $\mathcal{L}$ nodes are given by

$$[\Gamma] = \begin{bmatrix} . & 1 & & \\ 1 & . & & \\ & & \kappa & \\ & & . & \kappa \\ & & \kappa & . \end{bmatrix} \tag{A2}$$

where $\kappa = +1$ at a $\mathcal{P}$ node and -1 at an $\mathcal{L}$ node.

The corresponding matrices $[\Gamma]$ for the case when the plane of reflection symmetry (or line of rotational symmetry) is $x_1 = -x_2$ are obtained by multiplying the right-hand matrix of Eq. (A1) with that of Eq. (A2). For antisymmetric (or skew-symmetric) response, the right-hand sides of Eqs. (A1) and (A2) are multiplied by a minus sign.

References

[1] Chia, C. Y. and Prabhakara, M. K., "Post-Buckling Behavior of Unsymmetrically Layered Anisotropic Plates," *Journal of Applied Mechanics*, March 1974, pp. 155-162.

[2] Turvey, G. J. and Wittrick, W. H., "The Large Deflection and Postbuckling Behavior of Some Laminated Plates," *Aeronautical Quarterly*, May 1973, pp. 77-86.

[3] Schmit, L. A. and Monforton, G. R., "Finite Deflection Discrete Element Analysis of Sandwich Plates and Cylindrical Shells with Laminated Faces," *AIAA Journal*, Vol. 8, Aug. 1970, pp. 1454-1461.

[4] Stein, M. and Starnes, J. H., Jr., "Numerical Analysis of Stiffened Shear Webs in the Post-Buckling Range," *Numerical Solution of Nonlinear Structural Problems*, Applied Mechanics Division, ASME, Vol. 6, 1973, pp. 211-223.

[5] Almroth, B. O., Brogan, F. A., and Marlowe, M. B., "Collapse Analysis for Shells of General Shape, Vol. I - Analysis," Technical

Rept. N73-16916, AFFDL TR-71-8, Air Force Flight Dynamics Lab., Wright-Patterson Air Force Base, Ohio, 1973.

[6]Harris, G. Z., "The Buckling and Post-Buckling Behavior of Composite Plates Under Biaxial Loading," *International Journal of Mechanical Sciences,* Vol. 17, No. 3, March 1975, pp. 187–202.

[7]Harris, G. Z., "Buckling and Post-Buckling of Orthotropic Laminated Plates," Paper 75-813, Denver, Colo., 1975.

[8]Noor, A. K. and Mathers, M. D., "Anisotropy and Shear Deformation in Laminated Composite Plates," *AIAA Journal,* Vol. 14, Feb. 1976, pp. 282–285.

[9]Noor, A. K. and Mathers, M. D., "Nonlinear Finite Element Analysis of Laminated Composite Shells," *Computational Methods in Nonlinear Mechanics,* The Texas Institute for Computational Mechanics, Austin, Texas, Sept. 1974, pp. 999–1009.

[10]Glockner, P. G., "The Use of Symmetry and Group Theory in Structural Mechanics," Research Rept. CE 74-10, Dept. of Civil Engineering, The University of Calgary, Calgary, Canada, June 1974.

[11]Hamermesh, M., "Group Theory and Its Application to Physical Problems," Addison-Wesley, Reading, Mass., 1962.

[12]Noor, A. K. and Mathers, M. D., "Finite Element Analysis of Anisotropic Plates," *International Journal for Numerical Methods in Engineering,* Vol. 10, 1976, to be published.

[13]MacNeal, R. H. (ed.), "The NASTRAN Theoretical Manual," NASA SP-221, Sept. 1970.